Robot Trajectory Optimization for Safe Transport of Deformable Packages

Rishabh Shukla[1], Samrudh Moode[1], Fan Wang[2], Siddharth Mayya[2], and Satyandra K. Gupta[1]

Abstract— **Efficient and safe transport of deformable packages using suction cups is crucial in warehouse automation. Unlike rigid packages, deformable packages exhibit complex oscillatory behaviors and can detach under aggressive motions. Traditional motion planners typically overlook these oscillations, often resulting in either unsafe trajectories or overly conservative, slow motions. This paper addresses that gap by formulating package oscillation dynamics as constraints and incorporating them into a Cartesian trajectory optimization framework. These constraints are formulated to be state-dependent - i.e., they adapt according to the instantaneous conditions along the planned trajectory (such as acceleration and gripper orientation) - to ensure that oscillations remain within safe limits. We derive a pendulum-like model to characterize package swing, enforcing constraints on peak oscillation angles. Our approach then optimizes end-effector trajectories under these state-dependent constraints, ensuring safe transport when the end-effector follows constant-acceleration profiles. Real-world experiments demonstrate that our optimized trajectories reduce transport time by up to 18% compared to baseline motions while strictly adhering to safety limits on package swing.**

I. Introduction

In today's fast-paced e-commerce and manufacturing environments, efficient robotic manipulation of packages has become a critical necessity. The combination of rising demand for same-day deliveries [1], [2], increasing labor shortages in distribution centers [3], and the operational goal of minimizing cycle times [4] drives the push for automation. Robots equipped with diverse end-effectors, such as suction cups, are regularly deployed to pick and place items ranging from rigid boxes to soft or irregularly shaped packages [5], [6]. While motion planning for rigid payloads is well studied [7]–[9], many real-world packaging materials are deformable, introducing additional complexities in safe transport and motion generation.

Unlike rigid objects, deformable packages exhibit shape changes under load, making them susceptible to swing, oscillations, and partial detachments at higher velocities or accelerations [10], [11]. For example, many deformable packages can detach from suction cups due to inertial forces if robot motions are too aggressive [12]. In many existing robotic operations, operators revert to conservative trajectories with low accelerations to avoid damaging packages or risking drops [13], [14], resulting in slower overall throughput. Such an approach, though safe, is increasingly at odds with the need for rapid fulfillment, highlighting the importance of strategies that can model and limit oscillation while maintaining high-speed transport.

[1]Realization of Robotic Systems Lab, University of Southern California, Los Angeles, CA, USA. [2]Amazon Robotics, North Reading, MA, USA. Emails: {fanwanf, sidmayya}@amazon.com

Address all correspondence to guptask@usc.edu

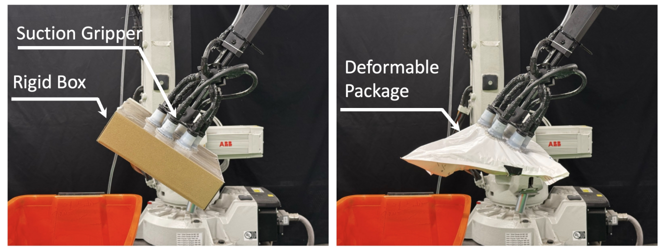

Fig. 1: Comparison of transport dynamics: (A) a rigid package with minimal oscillation versus (B) a deformable package exhibiting significant swing, motivating state-dependent oscillation constraints.

In our prior study [12], we optimized suction-based grip safety to avoid package detachment, enabling faster cycle times for certain deformable packages. We observed that constraints are inherently state-dependent. Conventional time-optimal path planning approaches, such as TOPP-RA [15], Graph of Convex Sets [16], and classic Bobrow's method [17], can yield near-minimum-time solutions; however, they do not consider dynamic, state-dependent, acceleration-based constraints arising from the payload's behavior, such as package oscillations, as illustrated in Fig. 1.

In this work, we propose a motion planning approach that explicitly models and limits package oscillations during transport. The key contributions of our approach are as follows: (1) We derive an analytical pendulum-like model for the package's oscillatory behavior and incorporate it as a constraint in a Cartesian trajectory optimization framework. Notably, the oscillation constraints are state-dependent – they automatically adjust based on the robot's instantaneous acceleration and orientation, ensuring the package's swing remains within safe bounds at all times. We calibrate the pendulum model's parameters using motion capture data from real robot movements, which improves the accuracy of oscillation predictions for various deformable packages. (2) Using this model, our trajectory optimizer generates smooth, constant-acceleration motion profiles for the robot's end-effector that respect the oscillation constraints. In doing so, the planner can push for faster speeds when possible, but will restrict accelerations or change orientation when the model predicts excessive swing. (3) We demonstrate the effectiveness of the approach on real-world transport tasks. The optimized trajectories reduce transport time by up to 18% compared to conservative baseline motions, all while maintaining the required safety margins for the package's stability (no drops or excessive oscillations observed).

II. Related Work

Research on deformable object manipulation has largely focused on developing either detailed models or data-driven policies for tasks such as cloth folding [18]–[20], rope disentangling [21], [22], and insertion or cutting operations [10], [11]. Simulation platforms like SoftGym [23] highlight the complexity of non-rigid dynamics by offering a suite of deformable tasks (cloth, rope, and fluid) to benchmark reinforcement learning approaches [24]–[26]. While these works provide valuable insights, particularly in learning control under uncertain material states, they often target relatively slow manipulations or cyclic tasks, such as iterative folding and smoothing [27], [28]. High-speed motion introduces a different risk profile: even brief accelerations can produce large swings or detachments [4], underscoring the need for trajectory planners that explicitly account for rapid oscillations in deformable packages.

On the time-optimal control side, foundational methods by Bobrow et al. [17] and subsequent extensions [15], [29] focus on respecting joint-level constraints—velocity, torque, or jerk—to minimize travel times. Approaches like TOPP-RA [15] efficiently parameterize the path for time-optimality but ignore the payload's dynamic response. Similarly, real-time trajectory generation methods [30], [31] and optimization-based planners such as CHOMP [32], TrajOpt [33], and sequential convex optimization [34] incorporate rich constraints (e.g., collision avoidance, smoothing) yet generally assume rigid payloads. As a result, these algorithms can produce trajectories that inadvertently exceed the safe dynamic envelope for a deformable item.

Motivated by the need for task-specific motion constraints, grasp-optimized frameworks have emerged. The GOMP family (GOMP [7], GOMP-FIT [8], and GOMP-ST [9]) shows how domain constraints (e.g., limiting accelerations to prevent spilling or suction failure) can significantly improve task performance. However, these methods assume a rigid payload and fail to address compliant systems. In compliant systems, payload flexibility can amplify oscillations, and traditional kinematic approaches do not address this issue. This necessitates an integrated model that can directly account for oscillatory behavior.

Our previous work [12] investigated safe, time-optimized transport of deformable packages using suction cups. The approach used a three-tier factor-of-safety prediction model to anticipate potential suction failures but did not explicitly model package oscillations. Consequently, as package deformation grew, the planner relied on empirical safety margins that could become overly conservative. In this paper, we extend the notion of coupling motion planning with a safety metric by integrating a pendulum-like model to capture and bound oscillatory behavior. Moreover, we employ both local and global solvers to systematically find optimal solutions subject to these oscillation constraints. This integrated framework not only refines the dynamic limits imposed on the trajectory but also enables a more balanced trade-off between speed and safety.

III. Problem Formulation

The primary objectives of this paper are twofold: (1) to develop a continuous and differentiable analytical model that accurately captures the complex oscillatory dynamics exhibited by deformable packages during robotic manipulation, and (2) to design a constraint-based, time-optimal trajectory planner that incorporates these dynamics as state-dependent constraints, ensuring the safe and efficient transportation of such packages.

Representing package safety constraints in Cartesian space provides a more direct and interpretable formulation. For example, one can directly bound the package's maximum lateral displacement, oscillatory amplitude relative to its nominal vertical alignment, or swing angle. Conversely, translating these constraints directly into joint space typically results in highly nonlinear, complex relationships that are challenging to enforce, interpret, and optimize.

Let the end-effector pose in Cartesian space be denoted as $\mathbf{p}(t) = (x, y, z, r_x, r_y, r_z)$. Our goal is to compute a time-optimal trajectory for the end-effector, moving a deformable package from an initial pose $\mathbf{p}_{\text{start}}$ to a desired final pose $\mathbf{p}_{\text{goal}}$. The trajectory must satisfy the following constraints:

1) **Robot Kinematic Constraints:**

$$\|\dot{\mathbf{p}}(t)\| \leq v_{\lim}, \quad \|\ddot{\mathbf{p}}(t)\| \leq a_{\lim},$$

where $\dot{\mathbf{p}}(t)$ and $\ddot{\mathbf{p}}(t)$ denote the velocity and acceleration vectors of the end-effector, respectively; $v_{\lim}$ and $a_{\lim}$ represent the robot's maximum allowable velocity and acceleration. These constraints ensure the end-effector operates within safe and achievable dynamic limits.

2) **Package Safety Constraint:**

$$f(\dot{\mathbf{p}}(t), \ddot{\mathbf{p}}(t)) \leq \beta_{\max},$$

restricting the induced sway or oscillations of the deformable package within specified safety thresholds. Here, $f(\cdot)$ represents a predictive function relating end-effector motion to measurable oscillation characteristics (e.g., angular deviation or lateral displacement), and $\beta_{\max}$ defines the permissible maximum oscillation. This function must capture effects induced by changes in end-effector velocity and acceleration while remaining continuous and differentiable. This property is crucial for enabling gradient-based solvers to efficiently find a feasible, locally optimal solution.

Formally, the problem can be posed as the following constrained optimization:

$$\begin{aligned}
&\min_{\mathbf{p}(\cdot)} T \quad \text{subject to:} \\
&\quad \|\dot{\mathbf{p}}(t)\| \leq v_{\lim}, \\
&\quad \|\ddot{\mathbf{p}}(t)\| \leq a_{\lim}, \\
&\quad f(\dot{\mathbf{p}}(t), \ddot{\mathbf{p}}(t)) \leq \beta_{\max}, \\
&\quad \mathbf{p}(0) = \mathbf{p}_{\text{start}}, \quad \mathbf{p}(T) = \mathbf{p}_{\text{goal}}.
\end{aligned}$$

IV. Approach

Our approach integrates an empirically calibrated pendulum-like oscillation model into a nonlinear Cartesian trajectory optimizer to ensure safe, high-speed transport of deformable packages. Figure 1 (in the Introduction) illustrated the motivation for these state-based constraints. The methodology follows four main steps:

A. Constraint Model for Predicting Package Detachment Risk

For small oscillation angles, we model the deformable package's swing as a pendulum attached to the end-effector. The static deflection of the package under a given horizontal acceleration a_i can be derived from simple pendulum physics: the package will hang at an angle $\arctan(a_i/g)$ (where g is gravity). The lateral displacement of the package (swing) is:

$$X_{m,i} = \ell \sin\Big(\arctan \frac{a_i}{g}\Big) \;=\; \ell \, \frac{a_i}{\sqrt{g^2 + a_i^2}}\,,$$

where ℓ is the effective length of the pendulum (distance from end-effector to package center of mass). This gives the steady-state offset of the package under acceleration a_i. The package's small oscillations about that offset can be approximated by simple harmonic motion. The natural frequency of the pendulum is:

$$\omega \;=\; \sqrt{\frac{g}{\ell}}\,.$$

We divide the robot's motion into two phases (e.g. accelerating and coasting). In each phase with roughly constant acceleration, the oscillation can be described as a sinusoid. We write the package sway $X(t)$ during phase i as:

$$X(t) \;=\; X_{m,i} + A_i\, e^{-\zeta\,(t-t_i)}\, \sin\Big[\omega\,\big(t - t_i\big) \;+\; \phi_i\Big],$$

Here $X_{m,i}$ is the steady deflection under the phase's acceleration a_i. ζ is the damping coefficient. The constants A_i and ϕ_i are the oscillation amplitude and phase at the start of that phase (time t_i), determined by initial conditions (how much swing carried over from the previous phase). The swing velocity is given by $V(t) = \dot{X}(t)$.

When the motion transitions to a new phase j (say, switching from acceleration to constant velocity), we compute new initial conditions for the oscillation. Using continuity of position and velocity at the transition, we update the amplitude and phase for the next segment:

$$A_j = \sqrt{X_j^2 + \Big(\frac{V_j}{\omega}\Big)^2}\,,$$

$$\phi_j = 2\,\arctan\!\left(\frac{X_j}{A_j\,\omega + V_j}\right),$$

where X_j and V_j are the swing displacement and velocity at the end of the previous phase (and start of the new phase). This piecewise pendulum model allows the planner to predict how the package will swing during each segment of the trajectory given the robot's acceleration profile.

B. Motion Capture Data Collection and Parameter Estimation

To accurately characterize how deformable packages swing under various accelerations, we followed a four-step methodology as follows:

1) **Controlled Acceleration Profiles**:
   We begin by subjecting a range of deformable packages to a set of known, piecewise constant-acceleration motions under the robot's end-effector. For each experimental trial, the robot executes a simplified trajectory (e.g., accelerating horizontally at a constant rate a for a predetermined duration), then decelerating to a stop.
2) **Tracking Swing and Oscillation**: A motion capture (MoCap) system tracks package oscillations by using reflective markers placed around the package.
3) **Parameter Fitting**: The pendulum model (length ℓ, damping factors, or equivalent terms) is derived by matching observed oscillation dynamics. Specifically, we fit the natural frequency $\omega = \sqrt{\frac{g}{\ell}}$ so that the predicted swing angle under constant acceleration matches the empirical amplitude measured by MoCap (refer to IV-A).
4) **Regressor**: Real-world warehouses handle new items with varying masses, dimensions. To generalize, we employ Gaussian Process Regression (GPR):
   Feature Set and Training Data: We define an input feature vector $\mathbf{x}_i$ for package i comprising:

   $$\mathbf{x}_i = \big[\text{mass, dimension, initial sagging}\big],$$

   The target output y_i is the fitted effective length ℓ_i. We collect such $\{\mathbf{x}_i, \ell_i\}$ pairs from all trials, producing a training set $\mathcal{D} = \{(\mathbf{x}_i, \ell_i)\}_{i=1}^{N}$.
   GPR Model and Kernel Selection: We use a Gaussian Process prior

   $$\ell(\mathbf{x}) \sim \mathcal{GP}\big(m(\mathbf{x}),\, k(\mathbf{x}, \mathbf{x}')\big),$$

   with a mean function $m(\cdot)$ (often taken as zero or a linear function) and a covariance (kernel) function $k(\cdot,\cdot)$. A common choice is the squared exponential (RBF) kernel:

   $$k(\mathbf{x}, \mathbf{x}') = \sigma^2 \exp\Big(-\tfrac{1}{2\alpha^2}\|\mathbf{x} - \mathbf{x}'\|^2\Big),$$

   where σ^2 is a signal variance and α is a length scale. We learn these hyperparameters $\{\sigma^2, \alpha\}$ by maximizing the log marginal likelihood of the data $\mathcal{D}$.
   Hyperparameter Tuning and Validation: To prevent overfitting, we perform K-fold cross-validation (e.g., $K = 5$) on the training set. For each fold, we temporarily remove a subset of packages, train on the remainder, and evaluate RMSE on the held-out fold. By iterating this process and comparing performance, we find a kernel hyperparameter set that generalizes well. We then retrain the GPR on the full dataset using these optimal hyperparameters.

Predicting $\hat{\ell}$ for New Packages: At runtime, to estimate ℓ for a new package with feature vector $\mathbf{x}_*$, we compute:

$$\hat{\ell}_* = \mu(\mathbf{x}_*) \pm \kappa\sqrt{\mathrm{Var}\big(\ell(\mathbf{x}_*)\big)},$$

where $\mu(\mathbf{x}_*)$ is the GPR mean prediction and $\mathrm{Var}\big(\ell(\mathbf{x}_*)\big)$ is the predictive variance. In practice, we may use mean-only estimate, i.e. $\hat{\ell}_* \approx \mu(\mathbf{x}_*)$.
Once trained, for any new package with similar materials and geometry, we query the GPR with the package features $\mathbf{x}$ to obtain $\hat{\ell}$. Our motion planner then uses $\hat{\ell}$ in the pendulum-like dynamics (Section IV-A) to compute swing angles and ensure constraint satisfaction.

We now have a pendulum-like formulation that predicts the package's equilibrium deflection angle $X_{m,i}$ for a given horizontal acceleration a_i, as well as its maximum swing amplitude for typical acceleration phases.

C. Trajectory Optimization with Oscillation Constraints

Finally, we integrate the above models and constraints into a trajectory optimization framework. We parameterize the robot's motion as a series of N segments with constant accelerations (piecewise constant acceleration profile). The decision variables in the optimizer include the duration of each segment (s_i) and the acceleration. The objective is to minimize the total transport time T.

We impose the following constraints in the optimization (applied for each segment i and overall trajectory):

- The velocity change in segment i is related to acceleration and time:

  $$a_i^x\, s_i = v_{i+1}^x - v_i^x,$$

  where s_i is the duration of segment i (and similarly for y/z axes if 3D).
- The position change over the segment accounts for acceleration and any coasting time within the segment:

  $$x_{i+1} - x_i = \Big(\frac{v_{i+1}^x + v_i^x}{2}\Big)s_i + v_{i+1}^x\,(t_d - s_i)\,.$$

  (Here t_d is the total duration up to the end of segment i, so if the segment doesn't last the full duration due to reaching a target velocity early, the remaining time is coasting at final velocity v_{i+1}.) At the start $(i = 0)$, we typically enforce:

  $$v_0^x = 0, \quad x_0 = x_{start}, \quad v_N^x = 0 \quad x_N = x_{goal}$$

  These equations enforce physically consistent motion for the end-effector's position x (and similarly for y, z, and 3D rotation).

Oscillation safety constraint: We divide the robot's motion into N segments of piecewise-constant acceleration $\mathbf{a}_i$. At the end of segment i, the package has a swing displacement X_i and a swing velocity V_i. We then require that

$$|X_i| \;\le\; \beta_{\max}, \quad \text{for } i = 1, \dots, N.$$

Here $\beta_{\max}$ is a predefined maximum allowable lateral swing angle (or displacement) based on safety requirements to avoid detachment.

To propagate from the end of segment $i-1$ to the end of segment i, we apply a pendulum-like model over the duration s_i with constant acceleration $\mathbf{a}_i$. We define a function $\mathcal{F}$ that encapsulates the pendulum's solution under constant acceleration for a time s_i as described in section IV-A. Symbolically,

$$\big(X_i,\, V_i\big) \;=\; \mathcal{F}\Big(X_{i-1},\, V_{i-1},\, \mathbf{a}_i,\, s_i\Big).$$

This update ensures continuity of the swing state from one segment to the next. If $\big|X_i\big| > \beta_{\max}$ for some trial solution, the optimizer must adjust $\mathbf{a}_i$ or s_i to reduce the package's swing by the end of that segment. By only evaluating X_i at these boundary points, we avoid a fully continuous-time swing constraint. This is less conservative than enforcing $|X(t)| \le \beta_{\max}$ at all times t, but it is considerably more tractable computationally. Because the mapping $\mathcal{F}$ involves trigonometric and exponential terms, the resulting constraints are nonlinear. Standard NLP solvers can handle these for a moderate number of segments N. In many industrial pick-and-place tasks, 3–10 segments are enough to capture the robot's accelerate–coast phases. This keeps the optimization dimension manageable while maintaining swing constraints that reduce or eliminate detachment risk.

We formulate the above as a nonlinear optimization problem. The objective is to minimize T (total time). We solve the resulting nonlinear trajectory optimization Sequential Quadratic Programming (SQP) , implemented via the Knitro solver. Knitro is a state-of-the-art nonlinear programming solver that can handle large numbers of variables and constraints efficiently, provided the functions are smooth and gradients are available. In our implementation, we supply analytical gradients for the objective and constraint functions (or use automatic differentiation) so that the solver can reliably navigate the search space. The SQP algorithm works by iteratively approximating the nonlinear problem as a quadratic sub-problem: at each iteration, it linearizes the constraints and approximates the objective by a quadratic, then solves this QP to propose a search direction, and finally performs a line search to update the solution. This process repeats until convergence criteria are met. We configure Knitro's parameters to ensure that the solver finds such a stationary point with high precision to obtain a locally optimal trajectory that achieves a good trade-off between speed and safety.

V. Results

In this section, we systematically evaluate the proposed motion planning framework under various scenarios designed to (i) validate the model for predicting package detachment risk, and (ii) demonstrate how incorporating the derived constraint enables faster, yet safe, end-effector trajectories.

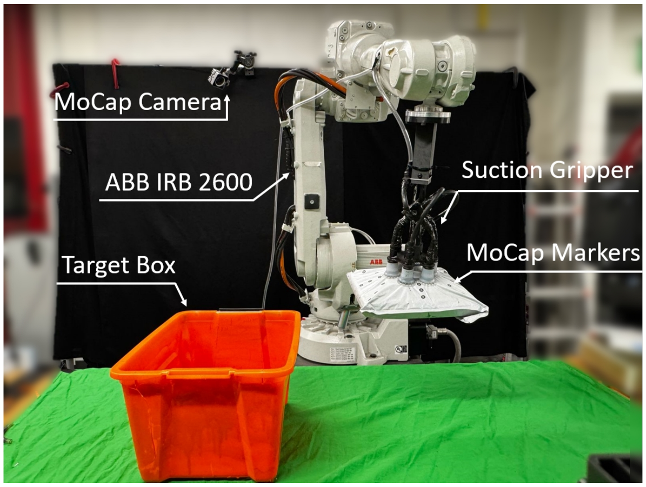

Fig. 2: Experimental setup featuring the ABB IRB 2600 165 robot with a suction gripper and MoCap tracking.

We first summarize the experimental setup and key metrics, then present detailed comparisons to baselines, followed by a series of ablation studies.

A. Experimental Setup

Cell Design: We conducted our experiments using an ABB IRB 2600 165 industrial robot equipped with a suction gripper powered by a vacuum pump. This gripper enables stable attachment of deformable packages of varying sizes and masses. The robot was programmed to follow predefined trajectories using the ROS2 framework. To accurately measure package oscillations, reflective patch markers were strategically placed on the surface of each package. A motion capture (MoCap) system tracked these markers in real-time at 240 Hz, providing precise oscillation measurements during the robot's motion. The experimental setup, including the placement of infrared markers on the package surface, is illustrated in Figure 2.

Package Specifications: In our study, we assume that the contents within the packages are tightly packed to minimize motion of the object inside the package. We make this assumption to simplify how inertial loading triggers grip failure. The packages used in our experiments vary in mass and the distance between the package edge and the nearest suction cup. The packaging material was the same for all packages. Table I categorizes these packages based on these properties.

	Mass	Suction-cup package edge distance →		
		6.5 cm	9 cm	10.25 cm
Training Phase	620 g	P1	P2	P3
	1020 g	P4	P5	P6
	1410 g	P7	P8	P9
Evaluation Phase	700 g	P10	P11	P12
	1200 g	P13	P14	P15

TABLE I: Experimental package specifications categorized by mass and suction-cup edge distance.

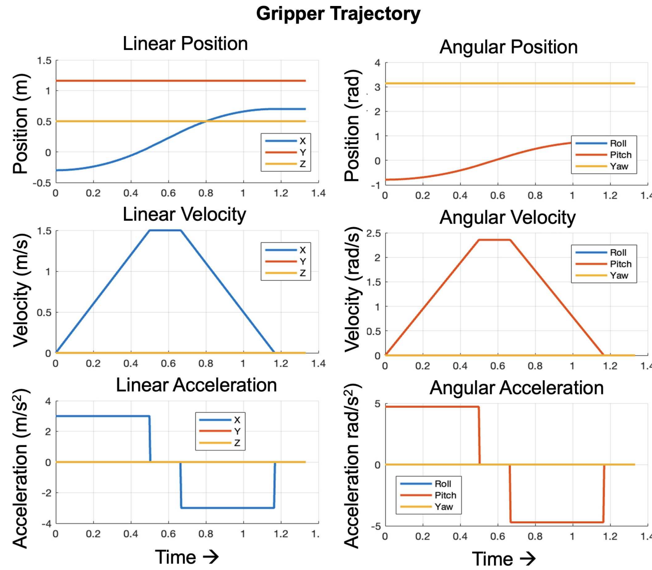

Fig. 3: Representative trajectory and acceleration profile used for data collection.

B. Data Collection

To accurately identify the oscillation model parameters for each package (e.g., effective pendulum length, damping factors), we designed a series of three geometric-constrained paths for the robot to follow. For each of these paths, we applied three distinct constant-acceleration profiles. Figure 3 shows one of the trajectories.

We used the following trajectory variations:

- *Geometric-Constrained Paths:* Each of the three paths is approximately 1.0–1.2 m in horizontal displacement with a 0.3 m vertical move. The end-effector's orientation remains within small angular deviations ($\pm 30°$) to reflect typical pick-and-place motions. The paths were chosen to cover short translational segments, gentle arcs, and simple vertical lifts.
- *Acceleration Profiles:* Along each geometric path, the robot executes three different constant-acceleration profiles. This variation elicits different dynamic responses from the deformable packages, enabling us to capture both minor oscillations and near-detachment scenarios.
- *Repeated Runs:* Each path-profile combination is repeated three times to reduce noise and outlier effects. Across nine package types, this procedure results in 243 total experiments.

C. Parameter Estimation

Using the experiments where the end-effector's orientation remained near-vertical, we fitted a Gaussian Process Regression (GPR) model as outlined in Section IV-B. Figure 4 plots the lateral oscillations over time for three packages (P3, P6, and P9) that share identical dimensions but differ in mass (620 g, 1020 g, and 1410 g). Each subplot shows the displacement of package from mean position in a fixed trajectory.

A key observation is that the oscillation frequency tends to increase as package mass increases. While a classical point-mass pendulum model suggests that frequency is independent

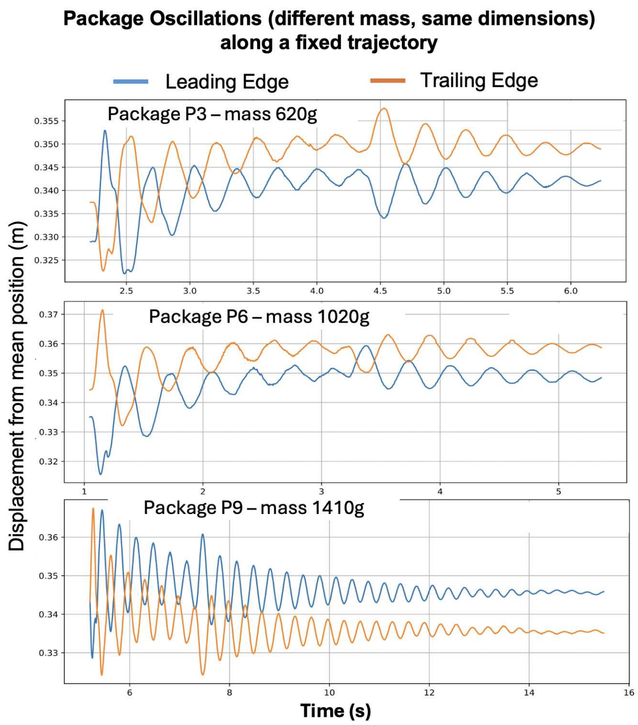

Fig. 4: Measured lateral displacements of the leading and trailing edges for three packages (P3, P6, and P9) that share identical external dimensions but vary in mass. Each subplot corresponds to the same end-effector trajectory. Notably, heavier packages show higher oscillation frequencies and more pronounced damping.

of mass, the real-world attachment and deformable packaging introduce an effective pivot and stiffness that vary with loading conditions. Here, lighter packages (e.g., P3) exhibit lower frequency compared to heavier ones (e.g., P9). We also note that heavier packages show more pronounced damping, so that the amplitude of oscillation decays faster over time. This can be seen in the bottom subplot for P9, where the initial swings start out fairly large but then settle more quickly relative to the total experiment duration.

From these experiments, we extract both the base pendulum parameters (ℓ, ζ) for each package and train the GPR on package-level descriptors (mass, dimensions). As mass increases, the estimated ℓ and damping ζ often shift accordingly, reflecting lower frequencies and higher energy dissipation. In the next sections, we use these refined parameters in our trajectory planner's oscillation constraints to improve transport safety for both light and heavy deformable packages.

D. Model Evaluation for Predicting Detachment Risk

A central objective of our work is to predict when a deformable package is at risk of detachment due to excessive oscillations. We propose that the maximum oscillation angle (or lateral swing) serves as a key indicator of detachment risk, and we validate this hypothesis through a series of controlled experiments.

We performed 25 motion trials, each combining different velocities (up to 1.8 m/s) and accelerations (up to 4.0 m/s^2). For each trial, we recorded the maximum observed swing angle via MoCap and noted whether a partial or full detachment occurred. Table II groups these trials into angle buckets and shows how often detachments occurred in each range.

Angle Range	No Detach (Count)	Detach (Count)	% Success
$< 8°$	6/6	0/6	100%
8°–16°	8/11	3/11	72%
$> 16°$	1/8	7/8	12.5%

TABLE II: Observed detachments across 25 trials, grouped by maximum swing angle. Zero detachment occurred below 8°, whereas most occurred above 16°.

From Table II, trials with low peak angles ($< 8°$) seldom detached, while large swings ($> 16°$) produced a significantly higher rate of failure. This strongly suggests that bounding the maximum allowed swing angle is a viable way to measure safety.

1) Threshold Analysis: To quantify how well a swing-angle threshold $\theta_{\max}$ predicts detachment, we vary $\theta_{\max}$ in the range 0–20° and classify each trial as "unsafe" if its measured peak swing $\geq \theta_{\max}$. Table III summarizes the corresponding True Positive Rate (TPR), False Positive Rate (FPR), and overall Accuracy for four representative thresholds: 8°, 16°, and 20°. We compute these metrics relative to the 10 actual detachments and 15 no-detach trials shown in Table II.

Threshold (°)	TPR (%)	FPR (%)	Accuracy (%)
8	100 (10/10)	60 (9/15)	64 (16/25)
16	70 (7/10)	6.7 (1/15)	84 (21/25)
20	20 (2/10)	0 (0/15)	68 (17/25)

TABLE III: True Positive Rate (TPR), False Positive Rate (FPR), and overall accuracy for various swing-angle thresholds, evaluated across 25 motion trials. TPR represents the fraction of actual detachments that were correctly predicted as unsafe, while FPR is the fraction of safe trials that were incorrectly flagged as unsafe.

We observe that lower thresholds (eg 8°) yield a perfect TPR but incur a high FPR; conversely, a very high threshold (20°) avoids false alarms but misses majority of detachment events, resulting in low accuracy. A threshold of $\theta_{\max} = 16°$ provides a balanced outcome with an 84% overall accuracy. From these results, we conclude that limiting the maximum package swing to around 16° is a practical way to ensure a high success rate while avoiding excessive false alarms. This corroborates the earlier observation in Table II that large swing angles ($> 16°$) are highly correlated with detachment events.

E. Comparative Evaluation of Trajectory Types

We evaluate our optimized trajectory against two baseline approaches:

- **Aggressive Trajectory**: A near-time-optimal solution that enforces only the robot's velocity and acceleration limits, ignoring package-swing constraints. This is prone to large oscillations and possible detachment.

- **Conservative Trajectory**: A slowed, low-acceleration approach that ensures that none of the packages detach. While it avoids detachment, this method sacrifices speed.
- **Optimized Trajectory**: Our method, which explicitly incorporates the specified package's oscillation constraints into the time-parameterized trajectory optimization. It seeks minimal transport time while guaranteeing swings $\theta_{\max} < 16°$).

F. Evaluation of Trajectory Optimization for Time Efficiency

To more systematically evaluate performance, we ran each of the three trajectory types on six different paths $\{\tau_1, \ldots, \tau_6\}$, each representing a distinct combination of horizontal/vertical displacements. Table IV reports the average execution times over three trials per path for a 1.2kg package. The optimized trajectory achieved an average time reduction of 18.3% (standard deviation: 7.9%) compared to conservative trajectories, while maintaining package oscillations safety limits.

Path	Aggressive (s)	Conservative (s)	Optimized (s)
τ_1	0.8	2.6	2.4
τ_2	0.8	2.7	1.9
τ_3	1.2	3.2	2.5
τ_4	0.9	2.8	2.3
τ_5	1.6	4.1	3.2
τ_6	1.4	2.7	2.4

TABLE IV: Execution times for three trajectory strategies across six representative paths. The Aggressive approach is fastest but prone to failures; Conservative never detaches but is slowest; Optimized respects $\theta_{\max} = 16°$ and remains significantly faster than Conservative while avoiding detachments.

G. Computation Time vs. Number of Segments

In our piecewise-constant-acceleration framework, the size of the NLP grows exponentially with N. Table V illustrates this effect for a representative pick-and-place scenario using an SQP-based solver (Knitro) on a desktop workstation (Intel Core i7 12th Gen CPU @ 3.2 GHz).

N	2	3	4	5	6	7	8
Solve Time (s)	5	6	8	25	40	95	175

TABLE V: Solver times vs. the number of segments N

Despite the steep increase in solve time, small N (e.g. 2–5 segments) is often sufficient for most industrial pick-and-place tasks (accelerate → coast → decelerate). Increasing N may produce a slightly better solution (lower total motion time) with increased computational cost.

VI. Conclusions

In this paper, we presented a motion-planning framework explicitly designed to incorporate deformable-package oscillation constraints into robot end-effector trajectory optimization. Our approach integrates empirical system identification of package-specific pendulum-like swing characteristics with a Gaussian Process Regression (GPR) model to generalize pendulum parameters across varying package masses and dimensions. Additionally, we introduced a state-dependent constraint enforcing a maximum allowable swing angle to ensure transport safety.

Experimental evaluations in real-world conditions confirmed the effectiveness of bounding the maximum oscillation angle (e.g., $\theta_{\max} = 16°$), reliably predicting and preventing grip failures. An analysis across 25 distinct motion trials identified a clear correlation between elevated swing angles and increased likelihood of package detachment. Comparative evaluations further demonstrated that aggressive trajectories, while faster, were highly susceptible to detachment, whereas conservative, low-acceleration trajectories ensured safety at the expense of substantial slowdowns. In contrast, our constrained optimization framework effectively balanced this trade-off, achieving an 18% reduction in transport time compared to conservative trajectories, all while maintaining a 100% success rate.

The robustness of our proposed framework was validated across a diverse range of package masses (620g to 1410g), effectively adapting to state-dependent conditions encountered during transport. These findings provide strong evidence that explicitly modeling oscillatory dynamics improves the operational efficiency without compromising safety.

Future work will focus on further refining oscillation models to better capture deformable package behavior, and on employing polynomial spline (e.g. cubic) trajectory formulations in order to generate smooth, dynamically consistent and safe trajectories.

Acknowledgment

This work is supported in part by Amazon Robotics. The opinions expressed are those of the authors and do not necessarily reflect the opinions of the sponsors.

References

[1] S. Ferguson, "Understanding america's labor shortage," Mar. 2024, U.S. Chamber of Commerce. [Online]. Available: https://www.uschamber.com/workforce/understanding-americas-labor-shortage

[2] K. Stevick, "Council post: Worker shortage: Overcoming workforce challenges in manufacturing," Aug 2023. [Online]. Available: https://www.forbes.com/sites/forbesbusinesscouncil/2023/08/25/worker-shortage-overcoming-workforce-challenges-in-manufacturing/?sh=20246b59250b

[3] G. Gow, "The labor shortage is killing american manufacturing. here's how ai can bring it back to life." Oct 2023.

[4] H. Pham and Q.-C. Pham, "Critically fast pick-and-place with suction cups," in *2019 International Conference on Robotics and Automation (ICRA)*, May 2019, pp. 3045–3051, iSSN: 2577-087X.

[5] J. Falco, K. V. Wyk, and K. Kimble, *Advances in Robot Technology Supporting Low-Volume/High-Mix Small Part Assembly Operations*. Recent Advances in Industrial Robotics, World Scientific Publishing Company (WSPC), Hackensack, NJ, 2022-01-25 05:01:00 2022.

[6] S. Baek and D. O. Kim, "Predictive process adjustment by detecting system status of vacuum gripper in real time during pick-up operations," *Processes*, vol. 9, no. 4, p. 634, 2021.

[7] J. Ichnowski, M. Danielczuk, J. Xu, V. Satish, and K. Goldberg, "Gomp: Grasp-optimized motion planning for bin picking," in *2020 IEEE International Conference on Robotics and Automation (ICRA)*, 2020, pp. 5270–5277.

[8] J. Ichnowski, Y. Avigal, Y. Liu, and K. Goldberg, "GOMP-FIT: Grasp-Optimized Motion Planning for Fast Inertial Transport," in *2022 International Conference on Robotics and Automation (ICRA)*, May 2022, pp. 5255–5261.

[9] Y. Avigal, J. Ichnowski, M. Y. Cao, and K. Goldberg, "GOMP-ST: Grasp Optimized Motion Planning for Suction Transport," in *Algorithmic Foundations of Robotics XV*, ser. Springer Proceedings in Advanced Robotics. Cham: Springer International Publishing, 2023.

[10] J. Zhu, A. Cherubini, C. Dune, D. Navarro-Alarcon, F. Alambeigi, D. Berenson, F. Ficuciello, K. Harada, J. Kober, X. Li *et al.*, "Challenges and outlook in robotic manipulation of deformable objects," *IEEE Robotics & Automation Magazine*, vol. 29, no. 3, 2022.

[11] F. Khalil and P. Payeur, "Dexterous Robotic Manipulation of Deformable Objects with Multi-Sensory Feedback - a Review," Mar. 2010.

[12] R. Shukla, Z. Yu, S. Moode, O. M. Manyar, F. Wang, S. Mayya, and S. K. Gupta, "Performing efficient and safe deformable package transport operations using suction cups," in *2024 IEEE/RSJ International Conference on Intelligent Robots and Systems (IROS)*. IEEE, 2024, pp. 11 835–11 842.

[13] N. Fangerow, D. Aschenbrenner, C. Colloseus, and R. Khoury, "Robot-assisted automated sorting techniques for plastic recycling," *Procedia CIRP*, vol. 120, pp. 1232–1237, 2023.

[14] S. Li, A. Keipour, K. Jamieson, N. Hudson, C. Swan, and K. Bekris, "Large-scale package manipulation via learned metrics of pick success," in *Robotics science and systems*. Robotics: Science and Systems, 2023.

[15] H. Pham and Q.-C. Pham, "A New Approach to Time-Optimal Path Parameterization Based on Reachability Analysis," *IEEE Transactions on Robotics*, vol. 34, no. 3, pp. 645–659, Jun. 2018, conference Name: IEEE Transactions on Robotics.

[16] T. Marcucci, J. Umenberger, P. Parrilo, and R. Tedrake, "Shortest paths in graphs of convex sets," *SIAM Journal on Optimization*, vol. 34, no. 1, pp. 507–532, 2024.

[17] J. Bobrow, S. Dubowsky, and J. Gibson, "Time-Optimal Control of Robotic Manipulators Along Specified Paths," *The International Journal of Robotics Research*, vol. 4, no. 3, pp. 3–17, Sep. 1985.

[18] D. Seita, P. Florence, J. Tompson, E. Coumans, V. Sindhwani, K. Goldberg, and A. Zeng, "Learning to rearrange deformable cables, fabrics, and bags with goal-conditioned transporter networks," in *IEEE International Conference on Robotics and Automation (ICRA)*, 2021.

[19] D. Seita, A. Ganapathi, R. Hoque, M. Hwang, E. Cen, A. K. Tanwani, A. Balakrishna, B. Thananjeyan, J. Ichnowski, N. Jamali *et al.*, "Deep imitation learning of sequential fabric smoothing from an algorithmic supervisor," in *2020 IEEE/RSJ International Conference on Intelligent Robots and Systems (IROS)*. IEEE, 2020, pp. 9651–9658.

[20] R. Lee, D. Ward, V. Dasagi, A. Cosgun, J. Leitner, and P. Corke, "Learning arbitrary-goal fabric folding with one hour of real robot experience," in *Conference on Robot Learning*. PMLR, 2021.

[21] J. Grannen, P. Sundaresan, B. Thananjeyan, J. Ichnowski, A. Balakrishna, V. Viswanath, M. Laskey, J. Gonzalez, and K. Goldberg, "Untangling dense knots by learning task-relevant keypoints," in *Proceedings of the 2020 Conference on Robot Learning*, ser. Proceedings of Machine Learning Research, vol. 155. PMLR, 16–18 Nov 2021, pp. 782–800.

[22] K. Shivakumar, V. Viswanath, A. Gu, Y. Avigal, J. Kerr, J. Ichnowski, R. Cheng, T. Kollar, and K. Goldberg, "Sgtm 2.0: Autonomously untangling long cables using interactive perception," in *2023 IEEE International Conference on Robotics and Automation (ICRA)*. IEEE, 2023, pp. 5837–5843.

[23] X. Lin, Y. Wang, J. Olkin, and D. Held, "Softgym: Benchmarking deep reinforcement learning for deformable object manipulation," in *Conference on Robot Learning*. PMLR, 2021, pp. 432–448.

[24] Y. Li, J. Wu, R. Tedrake, J. B. Tenenbaum, and A. Torralba, "Learning particle dynamics for manipulating rigid bodies, deformable objects, and fluids," in *ICLR*, 2019.

[25] P. Agrawal, A. V. Nair, P. Abbeel, J. Malik, and S. Levine, "Learning to poke by poking: Experiential learning of intuitive physics," *Advances in neural information processing systems*, vol. 29, 2016.

[26] J. Matas, S. James, and A. J. Davison, "Sim-to-real reinforcement learning for deformable object manipulation," in *Conference on Robot Learning*. PMLR, 2018, pp. 734–743.

[27] A. Nair, D. Chen, P. Agrawal, P. Isola, P. Abbeel, J. Malik, and S. Levine, "Combining self-supervised learning and imitation for vision-based rope manipulation," in *2017 IEEE international conference on robotics and automation (ICRA)*. IEEE, 2017, pp. 2146–2153.

[28] J. E. Hopcroft, J. K. Kearney, and D. B. Krafft, "A case study of flexible object manipulation," *The International Journal of Robotics Research*, vol. 10, no. 1, pp. 41–50, 1991.

[29] Q.-C. Pham, "A General, Fast, and Robust Implementation of the Time-Optimal Path Parameterization Algorithm," *IEEE Transactions on Robotics*, vol. 30, no. 6, pp. 1533–1540, Dec. 2014.

[30] R. Haschke, E. Weitnauer, and H. Ritter, "On-line planning of time-optimal, jerk-limited trajectories," in *2008 IEEE/RSJ International Conference on Intelligent Robots and Systems*, Sep. 2008, pp. 3248–3253, iSSN: 2153-0866.

[31] S. Macfarlane and E. Croft, "Jerk-bounded manipulator trajectory planning: design for real-time applications," *IEEE Transactions on Robotics and Automation*, vol. 19, no. 1, pp. 42–52, Feb. 2003, conference Name: IEEE Transactions on Robotics and Automation.

[32] N. Ratliff, M. Zucker, J. A. Bagnell, and S. Srinivasa, "Chomp: Gradient optimization techniques for efficient motion planning," in *2009 IEEE international conference on robotics and automation*. IEEE, 2009, pp. 489–494.

[33] J. Schulman, Y. Duan, J. Ho, A. Lee, I. Awwal, H. Bradlow, J. Pan, S. Patil, K. Goldberg, and P. Abbeel, "Motion planning with sequential convex optimization and convex collision checking," *The International Journal of Robotics Research*, vol. 33, no. 9, Aug. 2014.

[34] J. Schulman, J. Ho, A. Lee, I. Awwal, H. Bradlow, and P. Abbeel, "Finding Locally Optimal, Collision-Free Trajectories with Sequential Convex Optimization," in *Robotics: Science and Systems IX*, Jun. 2013.